Final Technical Report for 2017 USGS NEHRP Award G17AP00013

Thermomechanical Earthquake Cycle Simulations

PI: Eric M. Dunham
Department of Geophysics, Stanford University
397 Panama Mall
Stanford, CA 94305
(650) 725-6989, edunham@stanford.edu

Award Dates: 01/01/2017 to 12/31/2017

Abstract: The compositional and thermal structure and rheology of Earth's lithosphere determine how earthquakes occur in response to tectonic forcing. The depth extent of large earthquakes is controlled by the increase of temperature with depth, which leads to the transition from velocity-weakening to velocity-strengthening friction, and to the transition from frictional sliding on localized fault surfaces in the brittle upper crust to distributed crystal plastic creep (i.e., viscous flow) in the lower crust and upper mantle. The majority of earthquake cycle simulations neglect viscous flow, utilizing an elastic off-fault rheology and focusing solely on the frictional stability transition. However, such idealizations are inconsistent with geodetic observations of post- and interseismic viscous flow as well as laboratory constraints on rheology. To investigate interactions between distributed viscous flow at depth and frictional faulting in the seismogenic layer, we developed a simulation framework for earthquake sequences in viscoelastic solids with rate-and-state friction faults. Viscous flow is governed by temperature-dependent power-law dislocation creep laws, either using a fixed linear geotherm or, in the latest version of our code, a self-consistent and evolving temperature. The latter is based on simultaneous solution of the energy (i.e., heat) equation with two-way coupling to mechanics, with heating from frictional sliding and viscous flow decreasing effective viscosity and altering viscous strain rates. Major findings are as follows: 1.) Earthquake sequences are relatively insensitive to the nature of deformation at depth, at least for the rheological and frictional structure considered. This is because the depth extent of coseismic slip is bounded by the frictional stability transition, with stable, aseismic frictional sliding occurring over a region at least several kilometers deeper, prior to the onset of distributed viscous flow. The aseismic region thereby mediates stress transfer from flow or slip at depth to the seismogenic zone, and the nature of static elasticity is such that short-wavelength details of deformation at depth are lost. The form of the stress concentration that nucleates earthquakes at the base of the seismogenic layer is dictated by the aseismically slipping transition region. 2.) The deformation mechanism at depth is expressed in post- and interseismic deformation on Earth's surface, though predicted differences between models with various geotherms are relatively small and might be challenging to distinguish in real data. 3.) In simulations with fixed thermal structure, and laterally homogeneous rheologies, stress levels in the shallow upper crust far from the fault are predicted to be unrealistically high, for reasons explained later in this report related to rather high stresses occurring in the deep fault root. This suggests that processes which weaken fault roots, such as heating and thermomechanical feedback, grain size reduction, and foliation are required.

Publications and presentations supported by this award:

Allison, K. L., and E. M. Dunham (2017) Thermomechanical earthquake cycle simulations with rate-and-state friction and nonlinear viscoelasticity, Poster presented at Seismological Society of America Annual Meeting, Denver, CO, 18-20 April.

Allison, K. L., and E. M. Dunham (2017) Thermomechanical earthquake cycle simulations with rate-and-state friction and nonlinear viscoelasticity, Poster presented at Southern California Earthquake Center Annual Meeting, Palm Springs, CA, 9-13 September.

Allison, K. L., and E. M. Dunham (2017) Thermomechanical earthquake cycle simulations with rate-and-state friction and nonlinear viscoelasticity, Abstract G42A-07 presented at 2017 AGU Fall Meeting, New Orleans, LA, 11-15 December.

Allison, K. L., and E. M. Dunham (2017) Earthquake cycle simulations with rate-and-state friction and power-law viscoelasticity, Tectonophysics, doi:10.1016/j.tecto.2017.10.021.

Technical Report

Viscoelastic cycle simulations with fixed thermal structure: Our first study (Allison and Dunham, 2017) focused on earthquake cycle simulations in viscoelastic solids with the temperature distribution held fixed to some chosen geotherm (i.e., no thermomechanical coupling). Our model is similar to previous studies by Kato (2002) and Lambert and Barbot (2016), but those studies impose a priori the transition from frictional sliding to viscous flow, whereas that transition is determined as part of the solution in our approach. A schematic of the model is provided in Fig. 1, slip and viscous strain are shown in Figs. 2 and 3, and stress and effective viscosity profiles are shown in Figs. 4 and 5.

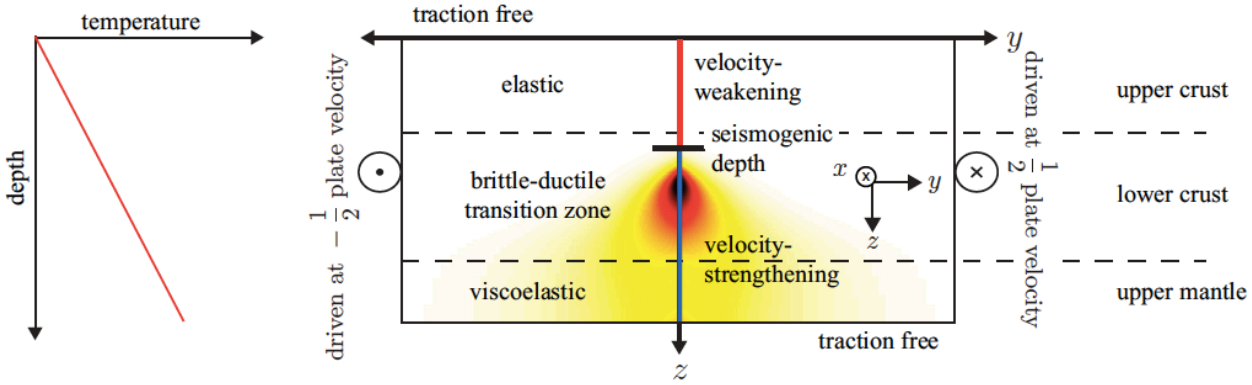

Fig. 1: 2D antiplane shear problem of a vertical strike-slip fault that transitions from velocity-weakening near Earth's surface to velocity-strengthening at depth. The increasing temperature with depth also causes on the onset of distributed viscous flow in the lower crust and upper mantle, indicated by the yellow/red colors. The system is driven at a constant plate velocity on the lateral boundaries. We use a quart-diorite flow law (Hansen and Carter, 1982; Freed and Burgmann, 2004) in the crust and wet olivine flow law (Hirth and Kohlstedt, 2003) in the mantle. From Allison and Dunham (2017).

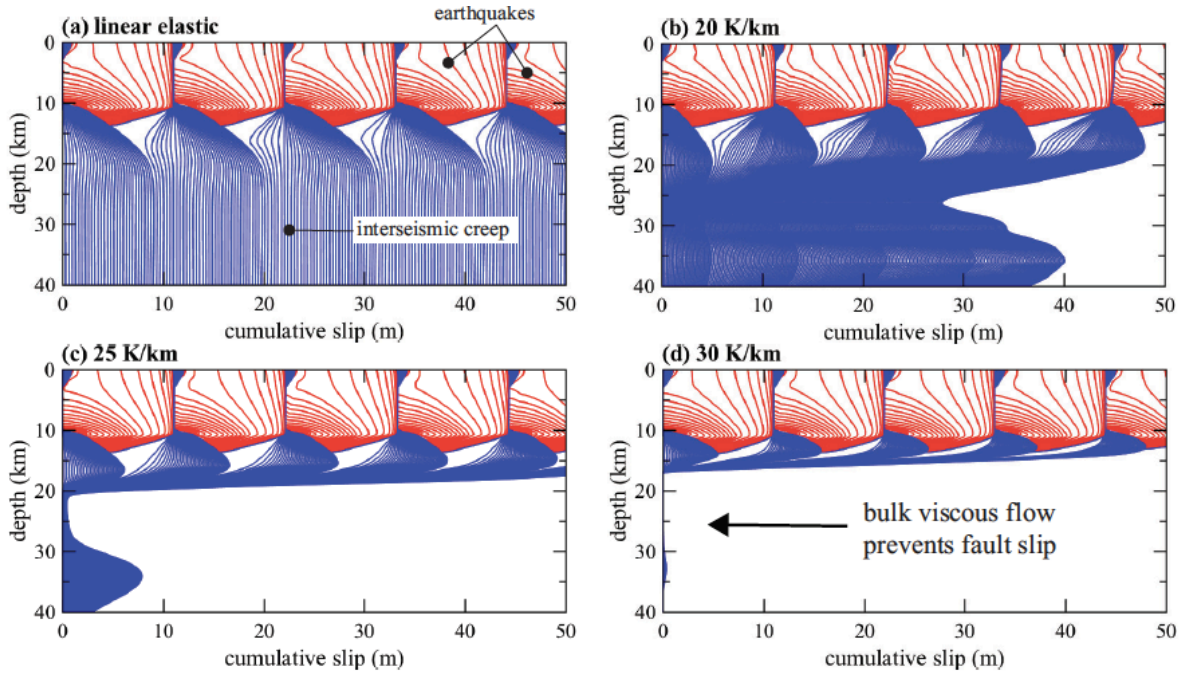

Fig. 2. Cumulative slip in (a) linear elastic and (b)-(d) viscoelastic models, the latter for fixed geotherms as labeled. Red curves show coseismic slip every 1 s, while blue curves are plotted every 10 yr. For the hotter geotherms, fault slip ceases below 17-20 km depth as the bulk material flow stress becomes smaller than the frictional stress required for slip. Note the similarity of coseismic slip, in terms of timing and amount, across all models. This is because loading of the seismogenic zone is mediated by aseismic fault creep over depths of 10 to ~17-20 km that is relatively similar for all models. The depth extent of ruptures is thus controlled by the frictional velocity-weakening to velocity-strengthening transition. From Allison and Dunham (2017).

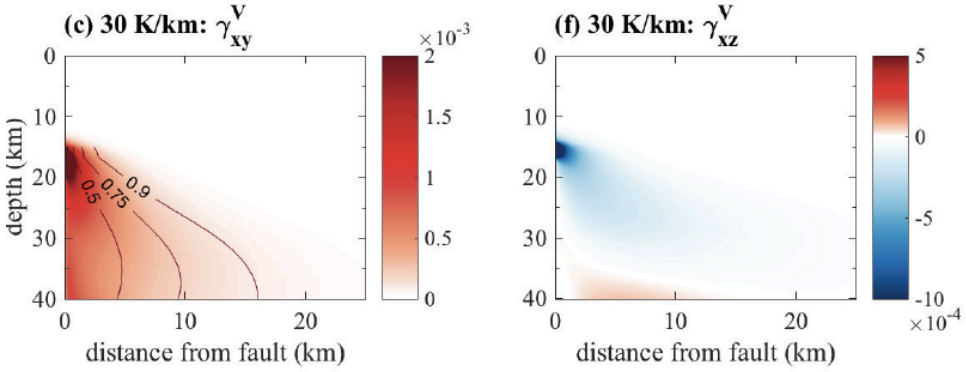

Fig. 3. Viscous strain accumulated over one earthquake cycle, for hottest geotherm (30 K/km). Left panel shows shear strain on vertical planes parallel to the fault; right panel shows shear strain on horizontal planes parallel to Earth's surface. Labeled contours in left panel indicate fraction of total viscous strain at that depth, which helps quantify the width of the ductile fault root. In the lower crust, the width is approximately 2-4 km, but broadens to ~5-10 km in the lower mantle. From Allison and Dunham (2017).

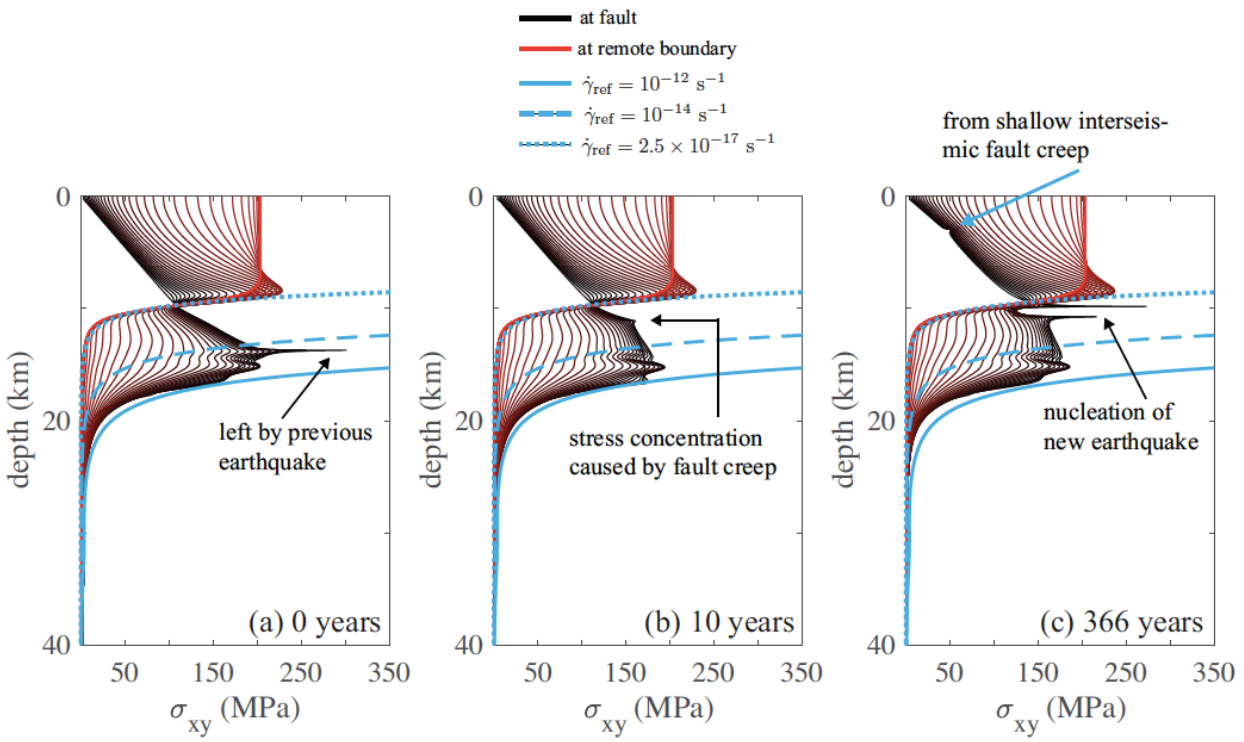

Fig. 4. Shear stress on vertical planes parallel to the fault, starting at the fault (black curve) and moving to the remote boundary (red curve), (a) immediately after the earthquake, (b) after the postseismic phase, (c) just prior to the next earthquake; all from 30 K/km model. Blue curves show predicted steady state viscous flow stress profiles for various assumed strain rates, for comparison. Close to the fault, stress increases approximately linearly with depth, consistent with relatively constant friction coefficient and linearly increasing effective normal stress. At depths of about 17-18 km, viscous flow begins and weakens the bulk in the lower crust and upper mantle. In contrast, far from the fault, where average strain rates are much lower, the stress is much lower and weakening from viscous flow happens at ~10 km depth. To balance forces within the crust, stress levels within the upper crust rise to unrealistically large values (~200 MPa near Earth's surface). Such high stresses would likely be prevented in the real Earth by formation of secondary faults or distributed inelastic deformation. Another possibility is that the ductile fault root might be weaker than predicted in this model due to grain size reduction and onset of diffusion creep, foliation and fabric development, or thermomechanical feedbacks. The stress reduction below the fault would then, through the overall force balance, decrease stresses in the upper crust away from the fault. From Allison and Dunham (2017).

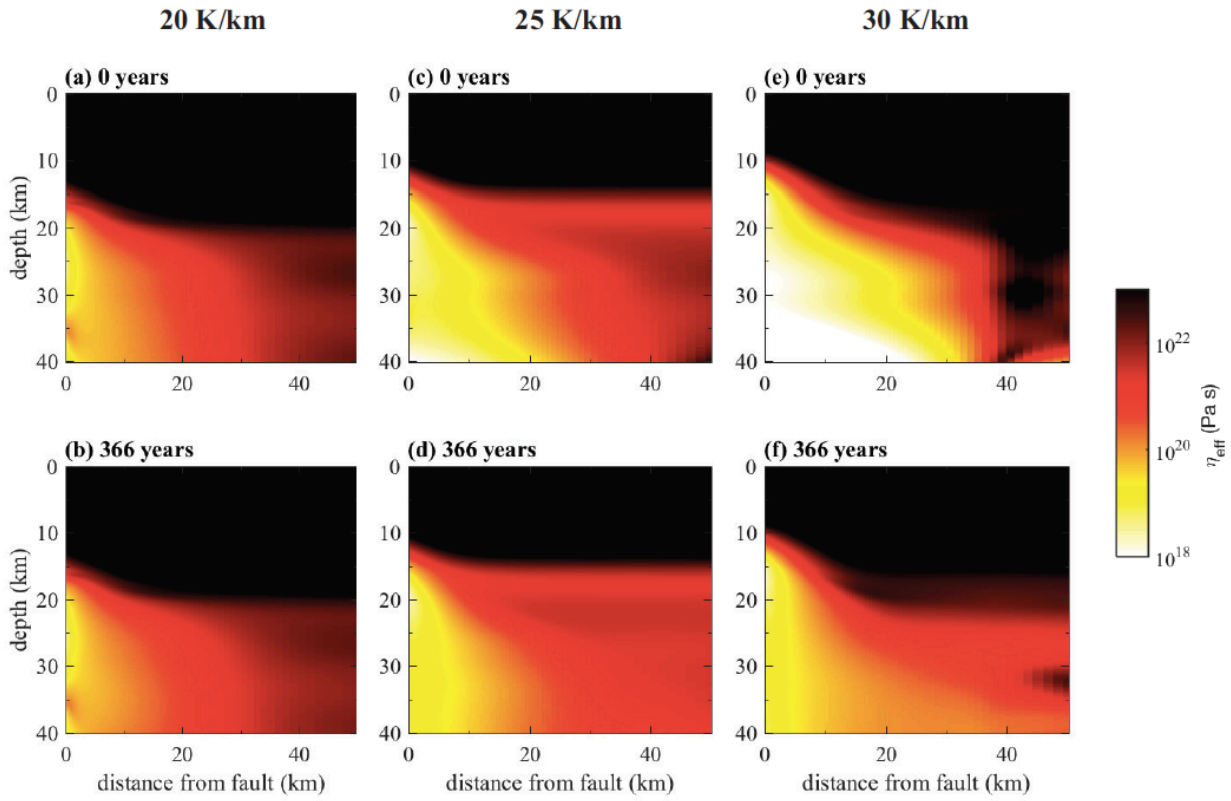

Fig. 5: Effective viscosity immediately after (top row) and just before (bottom row) an earthquake, for three different geotherms as labeled at top. All models show lower viscosity directly beneath the fault and extending ~10-20 km from it laterally. In the hotter geotherms, effective viscosity varies of several orders of magnitude throughout the earthquake cycle. Predicted viscosities are reasonably consistent with inferences from post- and interseismic deformation studies and xenoliths (e.g., Johnson et al., 2007; Thatcher and Pollitz, 2008; Behr and Hirth, 2014). From Allison and Dunham (2017).

Temperature evolution in the lithosphere: Following this first step, we added the energy equation to our simulation framework. Temperature obeys a diffusion equation (i.e., the heat equation) with source terms from frictional heating on the fault and distributed viscous flow. Initially we neglected temperature dependence in the flow law, so there is only one-way coupling to the energy equation. The primary purpose of this exercise was to investigate the temperature field, in particular to make sure our numerical method can resolve very thin thermal boundary layers surrounding the fault. To do this, we utilize an aggressive grid stretching technique that reduces grid spacing from ~10 to 100 m far from the fault down to less than ~1 mm. After extensive testing and verification of solution accuracy, we turned on thermomechanical coupling.

Thermomechanical coupling: Here we provide preliminary results on coupled thermomechanical simulations. The simulations only have shear heating from viscous flow and not from fault friction (though we have implemented that feature in our code). This is because with standard rate-and-state friction, without dynamic weakening or highly elevated fault pore pressure, unrealistically large amounts of heat are produced. (This is the well-known heat flow paradox.) We are exploring

models with dynamic weakening, but results are too preliminary to warrant reporting here. We performed a parameter space search in which we varied λ, the ratio of pore fluid pressure to lithostatic pressure (both increase linearly with depth). A value of λ=0.37 indicates hydrostatic pressure, and higher λ means pressures above hydrostatic. Fig. 6 shows the cycle-averaged temperature anomaly and shear stress resulting from viscous flow as a function of λ. The results are similar to those obtained by Takeuchi and Fialko (2012).

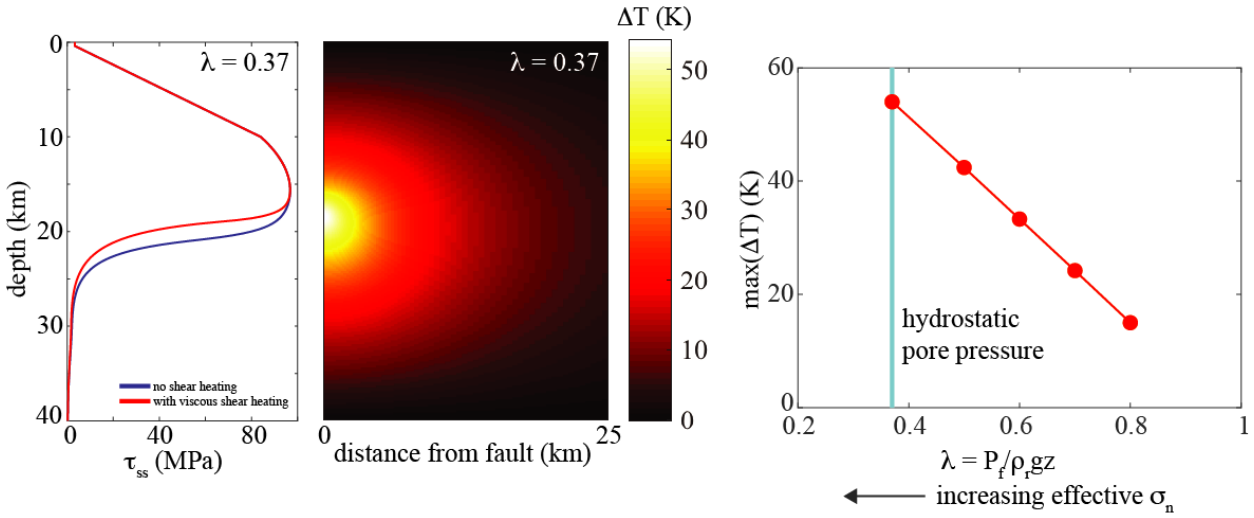

Fig. 6. Results from thermomechanically coupled simulations that account for effective viscosity reduction by increased temperatures from shear heating during viscous flow (but not fault frictional slip). (left) Shear stress on fault and the ductile fault root beneath it. Thermomechanical coupling (red curve) reduces stress in the lower crust relative to models neglecting coupling. (center) Temperature perturbation, showing an increase of over 50 K near the transition from frictional sliding to viscous flow. (right) Maximum temperature perturbation as a function of λ.

Plans for future work: Now that we have our fully coupled thermomechanical cycle code working, we will use it to study the importance (or not) of thermomechanical feedbacks. Like Takeuchi and Fialko (2012) we will do this first for models that neglect fault frictional heating to provide a baseline for comparison when we later enable it. Our hypothesis is that temperature increases in the ductile fault root will reduce stress, as already indicated in Fig. 6, perhaps even to the point that off-fault upper crustal stresses will drop to more realistic values than those shown in Fig. 4. It is possible that accounting for fault frictional heating will be necessary, as stress and hence heat production rate would be highest near the transition from frictional sliding to viscous flow.

We also plan to explore alternative rheologies for the ductile fault root. Many studies have argued that extensive shearing of this material leads to reductions in grain size, to the point where diffusion creep becomes the dominant deformation mechanism instead of dislocation creep as assumed thus far in our work. In addition, fabric or foliation structures might develop that reduce the flow stress (White et al., 1980; Montési and Zuber, 2002; Bürgmann and Dresen, 2008; Platt and Behr, 2011;; Montési, 2013).

References

Allison, K. L., and E. M. Dunham (2017) Earthquake cycle simulations with rate-and-state friction and power-law viscoelasticity, Tectonophysics, doi:10.1016/j.tecto.2017.10.021.

Behr, W. M., and G. Hirth (2014), Rheological properties of the mantle lid beneath the Mojave region in southern California, Earth and Planetary Science Letters, 393, 60-72, doi:10.1016/j.epsl.2014.02.039.

Bürgmann, R., Dresen, G., 2008. Rheology of the lower crust and upper mantle: evidence from rock mechanics, geodesy, and field observations. Annu. Rev. Earth Planet. Sci. 36 (1), 531–567. http://dx.doi.org/10.1146/annurev.earth.36.031207.124326.

Freed, A. M., and R. Burgmann (2004), Evidence of power-law flow in the Mojave desert mantle, Nature, 430 (6999), 548{551, doi:10.1038/nature02784.

Hansen, F., and N. Carter (1982), Creep of selected crustal rocks at 1000 MPa, EOS: Transactions American Geophysical Union, 63, 437.

Hirth, G., and D. 902 Kohlstedt (2003), Rheology of the upper mantle and the mantle wedge: A view from the experimentalists, in Inside the Subduction Factory, chap. 5, pp. 83-105, American Geophysical Union, doi:10.1029/138GM06.

Johnson, K. M., G. E. Hilley, and R. Burgmann (2007), Influence of lithosphere viscosity structure on estimates of fault slip rate in the Mojave region of the San Andreas fault system, Journal of Geophysical Research: Solid Earth, 112 (7), doi:10.1029/2006JB004842.

Kato, N. (2002), Seismic cycle on a strike-slip fault with rate- and state-dependent strength in an elastic layer overlying a viscoelastic half-space, Earth, Planets and Space, 54 (11), 1077-1083, doi:10.1186/BF03353305.

Lambert, V., and S. Barbot (2016), Contribution of viscoelastic flow in earthquake cycles within the lithosphere-asthenosphere system, Geophysical Research Letters, 43 (19), 10,142-10,154, doi:10.1002/2016GL070345.1.

Montési, L.G.J., Zuber, M.T., 2002. A unified description of localization for application to large-scale tectonics. J Geophys Res 107 (B3), doi:10.1029/2001JB000465.

Montési, L.G.J., 2013. Fabric development as the key for forming ductile shear zones and enabling plate tectonics. J. Struct. Geol. 50, 254–266, doi:10.1016/j.jsg.2012.12.011.

Platt, J.P., Behr, W.M., 2011. Deep structure of lithospheric fault zones. Geophys. Res. Lett. 38 (24), doi:10.1029/2011GL049719.

Takeuchi, C. S., and Y. Fialko (2012), Dynamic models of interseismic deformation and stress transfer from plate motion to continental transform faults, Journal of Geophysical Research: Solid Earth, 117 (B5), doi:10.1029/2011JB009056.

Thatcher, W., and F. F. Pollitz (2008), Temporal evolution of continental lithospheric strength in actively deforming regions, GSA Today, 18 (4/5), 4-11, doi:10.1130/GSATO1804-5A.1.

White, S., Burrows, S., Carreras, J., Shaw, N., Humphreys, F., 1980. On mylonites in ductile shear zones. J. Struct. Geol. 2 (1), 175–187, doi:10.1016/0191-8141(80)90048-6.